Design and Development of the *Atlas* Human-Powered Helicopter

Cameron Robertson
Cameron.Robertson@aerovelo.com
VP Structures

Todd Reichert
Todd.Reichert@aerovelo.com
VP Aerodynamics

AeroVelo Inc.
Toronto, ON, Canada

ABSTRACT

AeroVelo initiated the *Atlas* Human-Powered Helicopter Project in August 2011 to capture the AHS Sikorsky Prize, which despite prior attempts had remained unclaimed for over 30 years. A configuration study was undertaken using low-fidelity aerodynamic analysis and estimated mass figures. The authors developed an aero-structural optimization scheme for rotor design, including a novel vortex-ring aerodynamic model with included ground effect prediction, finite-element analysis and integrated composite failure analysis, and a detailed weight estimation scheme. The airframe was comprised of a wire-braced truss structure, and innovative designs were developed for many of the aircraft's lightweight-focused subsystems. After initial flight-testing in August 2012, experimental optimization and performance improvement led to a second testing program beginning in January 2013. Testing in 2013 led to a reduction in required power, improved understanding of structural dynamics and control strategy. The project culminated in a successful AHS Sikorsky Prize flight on June 13th, 2013.

INTRODUCTION

The American Helicopter Society (AHS) announced the Igor I. Sikorsky Human-Powered Helicopter Competition (colloquially the "AHS Sikorsky Prize") in 1980, with a prize of USD$20,000. This was an effort to spark innovation and excitement in the vertical lift community similar to that brought about for the fixed-wing community by the English Channel crossing of the Gossamer Albatross in 1979, the most accomplished human-powered aircraft to-date (Ref. 1). In the following 30 years there were many attempts but only a few brief flights of a human-powered helicopter (HPH). In 2009 Sikorsky Aircraft Corp. pledged USD$250,000 to the winner in order to re-invigorate the competition (Ref. 2).

The key requirements for a single prize-winning flight were as follows (Ref. 3):

1. The aircraft must be powered only by its human occupants;
2. The aircraft must remain aloft for 60 seconds;
3. All parts of the aircraft must momentarily exceed 3 *m* in altitude;
4. A reference point on the aircraft must remain inside a 10 *m* by 10 *m* box throughout the flight;
5. The rotation of the aircraft throughout the flight must not exceed 180 degrees;
6. The drive system could not utilize stored energy in any form.

These rules effectively required a helicopter that was extremely efficient (a human engine can produce only about 1 *hp* for a 60-second effort), and was controllable or at least stable and well-trimmed. As would be seen later, bringing all these aspects together in a single flight was perhaps the most daunting part of the challenge.

Between 1980 and 2011, despite 35+ projects achieving various stages of completion, there were only three HPHs to achieve flight (Ref. 4). In 1989, the *DaVinci III* at California Polytechnic Institute was the first to fly, achieving 8 *s* and a few inches of height (Ref. 5). This was a single-rotor helicopter with reaction-drive tip propellers. In 1994, the *Yuri I* was flown at Nihon University in Japan, again for inches of height but achieving up to 19 *s* duration (Ref. 6). *Yuri I* utilized a quad-rotor configuration. In 2011, the University of Maryland began to fly *Gamera I* (also quad-rotor), achieving duration up to 11.4 *s* (Ref. 7). Team Gamera undertook comprehensive redesign and optimization to produce the much-improved *Gamera II* in 2012 (Ref. 8). A summary of the specifications of these successful aircraft is available in table 1.

PROJECT ORIGIN AND TIMELINE

The *Atlas* Human-Powered Helicopter Project was started in fall 2011. Reichert and Robertson had led the team that designed, built, and flew the *Snowbird* Human-Powered

Presented at the AHS 70th Annual Forum, Montréal, Québec, Canada, May 20–22, 2014. Copyright © 2014 by the American Helicopter Society International, Inc. All rights reserved.

Table 1. Specifications of Prior Successful HPHs (Refs. 5–7).

Specification	*DaVinci III*	*Yuri I*	*Gamera I*
Rotors	1	4	4
Drive System	Tip-Props	String Drive	String Drive
Rotor Dia.	100 *ft*	32.8 *ft*	49.2 *ft*
Rotor RPM	8.6	22.2	18
Empty Weight	97.2 *lb*	70.5 *lb*	107.0 *lb*
All-Up Weight	225.5 *lb*	191.8 *lb*	214.0 *lb*
Hover Power	640 *W*	398 *W*	600 *W*

Ornithopter, which in 2010 became the World's first successful piloted flapping-wing aircraft. This aircraft had required development of lightweight composite structural design and fabrication techniques, advancements in HPA construction, and unique models for aerodynamic analysis and multi-disciplinary optimization techniques (Refs. 9–11). This prior work laid the foundation for the design of *Atlas*.

The *Atlas* Project was conducted over two years, with milestones listed in table 2.

Table 2. *Atlas* Project Timeline

2011, August	Feasibility Study and literature review.
2012, January	Focused design trade-off studies and engineering model development.
2012, May	Configuration & rotor design freeze, begin design & fabrication stage.
2012, August	Airframe integration and initial flight-testing.
2012, October	Experimental optimization and modifications of airframe.
2013, January	Resumed weekly flight-testing and continuous improvement (major crashes in March & April).
2013, June	Flight-testing session culminating in Sikorsky Prize flight on June 13.
2013, September	Final flight-testing and endurance record attempts.

CONFIGURATION STUDY

The initial literature survey suggested that a successful helicopter would be very large, with a main rotor as much as 150 *ft* in diameter (Ref. 4). This was crucial to take advantage of the reduced power requirements of an extremely low disc-loading and increased ground-effect.

The initial configuration study evaluated quad-rotor, counter-rotating, single-rotor/tip-reaction drive, and single-rotor/tail-rotor arrangements with and without hinged blades. The primary objective was to compare the required power of candidate designs for each configuration. A low-fidelity aerodynamic analysis based on actuator disk and blade element theory was derived based on Bramwell (Ref. 12). Each candidate design assumed linear distributions of chord $c(x) = c_0 - c_1 x$, lift coefficient $C_l(x) = C_{l0} - C_{l1} x$, and drag coefficient $C_d(x) = C_{d0} - C_{d1} x$, with the resulting power given by

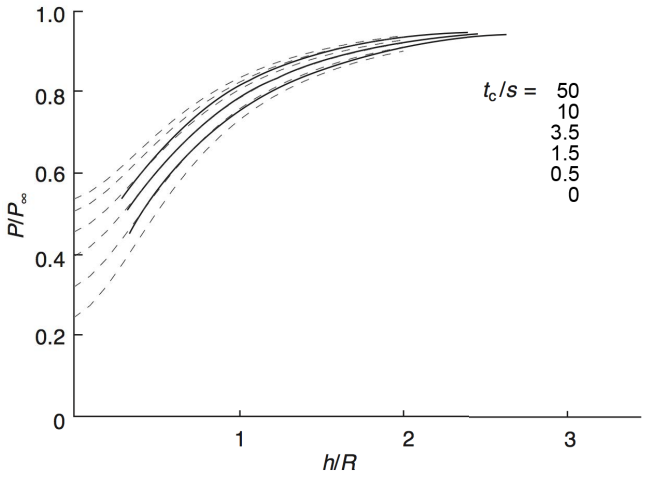


Fig. 1. Ground effect curves from Bramwell extrapolated below $h/R = 0.3$.

$$P = \frac{1}{2}\rho b \Omega^3 R^4 \left(\frac{1}{4} C_{d0} c_0 - \frac{1}{5} C_{d0} c_1 - \frac{1}{5} C_{d1} c_0 + \frac{1}{6} C_{d1} c_1 \right) + k_i k_g T v_i \quad (1)$$

where the first term in the resulting formula is the profile power and the second term is the induced power; Ω is the angular velocity, R is the rotor radius, ρ the atmospheric density, b the number of blades, and v_i the induced downwash given by

$$v_i = \sqrt{\frac{T}{2\rho A}} \quad (2)$$

The constant k_i reflects the extent to which the rotor has attained an ideal, constant, downwash, and varies from 1 for and ideal rotor to 1.13, as given by Bramwell for a more typical rotor. The constant k_g represents the reduction in induced power due to ground effect. For the purpose of the configuration study k_g was determined from curve fitting Bramwell's analytic results for h/R between 0 and 1. Bramwell's data is only presented above $h/R = 0.3$, and given the unknowns with lightly loaded rotors in deep ground effect, a highly-conservative extrapolation was used to estimate k_g below this threshold (see figure3).

Blade element C_d was estimated based on a method by Hoerner, that uses only airfoil thickness t, chord, Reynolds number and % laminar flow on the top and bottom surfaces. The method is summarized in Tamai's Leading Edge, and allows for a parametric analysis and optimization of the rotor radius and chord without having to select a specific airfoil and a specific Reynolds number (Ref. 13).

Validation of the model used X-FOIL results for the series of NACA 66-2xx airfoils, where xx refers to airfoils of different thickness, all designed for a lift coefficient of 0.2. The model was found to provide an excellent first approximation, capturing trends in Reynolds number and airfoil thickness as shown in figure 2. Slight disagreement was found for

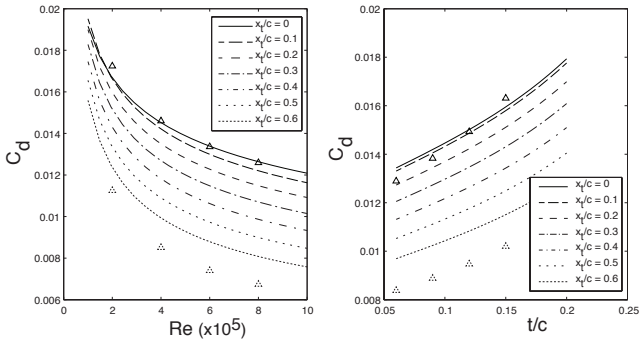


Fig. 2. Validation of Model by Tamai for C_d Estimation with X-FOIL test points. x_t/c is the chord-fraction of the forced laminar-turbulent transition location.

Table 3. Cyclist Specific-power capabilities [W/Kg].

Category	Male	Female
Untrained	5.99	4.94
Good (Cycling Cat. 3)	8.17	6.66
Excellent (Cycling Cat. 1)	9.66	7.84
World-Class Professional	11.04	8.93

airfoils with increased runs of laminar flow. This profile drag model was also used in the later higher-fidelity optimizations until superseded by X-FOIL data for the custom-designed BE-series HPH airfoils (designed by Brian Eggleston), used in the last stage of optimization.

For the initial structural model, mass parameters and total weight prediction were estimated from empirical data based on previous HPHs and on the authors' previous HPA experience.

One of the initial design ideas prompted an investigation of utilizing a hinged rotor system. An estimate for the resulting coning angle was based Bramwell, and expanded to accommodate a linearly varying blade mass, $m(x) = m_0 - m_1 x$, and tip weight m_{tip}. The derived equation for coning angle β is

$$\beta = \frac{\frac{1}{2}\rho\left(\frac{1}{4}C_{l0}c_0 - \frac{1}{5}C_{l0}c_1 - \frac{1}{5}C_{l1}c_0 + \frac{1}{6}C_{l1}c_1\right)R}{\left(\frac{1}{3}m_0 - \frac{1}{4}m_1\right) + m_{tip}/R} \qquad (3)$$

with linearly varying chord and lift coefficient, $c(x) = c_0 - c_1 x$ and $C_l(x) = C_{l0} - C_{l1}x$, rotor radius R, and air density ρ. Immediately the result of this estimation scheme was that a hinged HPH rotor would be excessively heavy, of a very small chord, and required 5 kg tip weights to maintain a reasonable coning angle. This was deemed practically infeasible.

Finally, a power estimate was required for the human engine. The Peak Centre for human performance provided power estimates for several categories of male and female athletes over a 1 minute effort (table 3) (Ref. 14). The World-Class and Good category powers were used to define the potential expected power envelope for this design study.

In retrospect these figures accurately illustrated the difficulty of the Sikorsky Prize: the *Atlas's* winning flight required

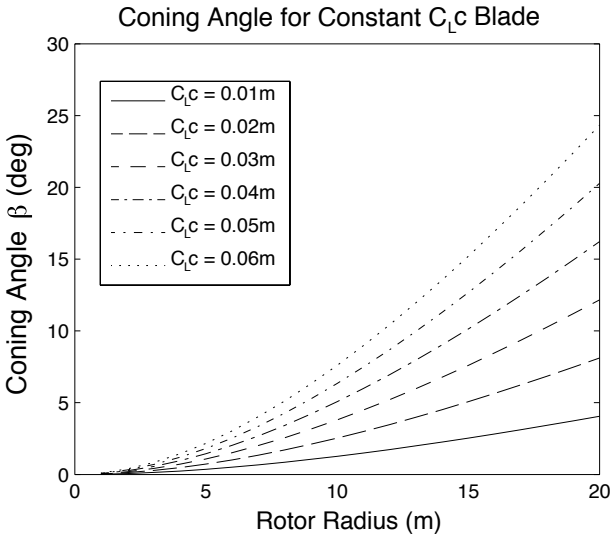


Fig. 3. Resulting coning angle at various C_{Lc} values, for a blade with a mass of 0.5 kg/m and a tip mass of 5 kg.

Table 4. Specifications for Early Configurations Evaluated

Parameter	Prop Driven	Counter Rotating	Hinged CR	Quad Rotor	Hinged QR	Tail Rotor
Weight [lbs]	70	100	80	100	100	70
Radius [ft]	52	46	49	25	25	52
Rotor Height [ft]	5	5	20	0.3	11	5
k_i	0.6	0.6	0.7	0.6	0.7	0.6
β [deg]	5	10	30	5	28	5

an average power of about 690 W, which for the 70 Kg pilot is 9.85 W/Kg, that of a semi-professional athlete. Key specifications of each of the evaluated configurations are given in table 4 (with k_i the expected fraction of the ideal inflow velocity).

The results of the analysis for each configuration are presented in figure 4. Each configuration was compared for required power versus altitude, with the blue and red lines defining the power expected from male and female "Good" and World Class athletes. The hinged and tail-rotor configurations were discarded due to substantially higher power requirements. At this stage, the counter-rotating configuration was also removed due to operational risk (rotor collisions) and mechanical complexity, elements that had abruptly ended the *Thunderbird* Project at University of British Columbia (Ref. 4).

Similar power requirements and lack of substantial disadvantages preserved the reaction-drive single-rotor and quad-rotor designs for further study. The quad rotor configuration was known to be capable of stable flight (from prior HPHs) and utilized structures technology within the project team's level of expertise. Two important early conclusions were

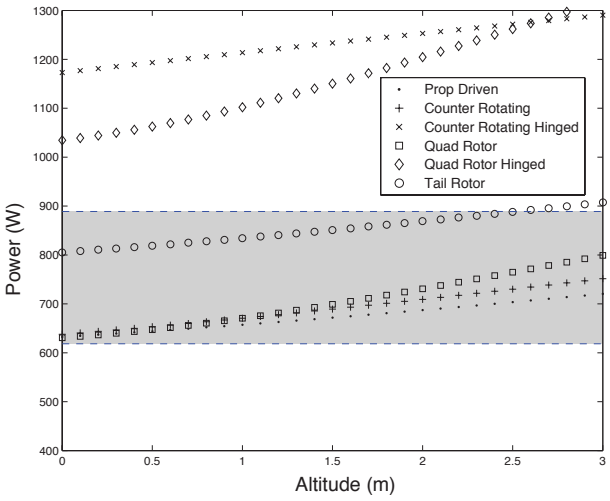


Fig. 4. Plot of power versus altitude for candidate configurations, with power available from a good to World-class male athlete indicated by grey band.

drawn that would guide the next stage. First, a rotor construction method that prioritized lightweight (similar to the Gossamer Albatross) over aerodynamic refinement (similar to that used for *Snowbird*) would ultimately require less power. Second, both remaining configurations showed an optimum size that was larger than expected, but with a required power lower than expected.

Rotor Design Methodology

An aero-structural optimization scheme `HeliCalc` was developed for follow-on rotor detailed design and final configuration selection. Medium-fidelity aerodynamic and structural models were developed with the goal of having a computationally inexpensive design code that could be used to quickly navigate the design space and compare various 'optimal' configurations. From the authors' previous experience on the design of the *Snowbird* it was decided that gradient-based optimization would play a major role in the design process and, as such, much attention was paid to ensure that the computational models produced smooth and continuous outputs with changes in the design variables.

The aerodynamic model included the option to use a simpler blade element model, or the more advanced vortex ring model. The blade-element model was extended to allow any prescribed distribution of C_L, C_D, and c, as well as a more accurate ground effect models by Cheeseman and Bennett, as well as Hayden that predicted the reduction in induced power down to zero altitude (Refs. 15, 16).

The vortex ring model was inspired by the work of Rayner on the hovering flight of birds and bats, where the complex aerodynamics of a single wing beat and simplified as the shedding of a single discrete vortex ring (Ref. 17). Further on in the project it was found that a similar vortex-emitter concept

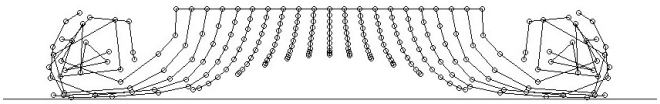


Fig. 5. A cross-section of the vortex wake, where each circle represents and planar vortex ring, with strength and direction dependent of the circulation distribution of the rotor.

had been used by Brand et al in the investigation of vortex-ring state in helicopters (Ref. 18). In the case of a helicopter, the helical 3-D structure of the wake is flattened into a series vortex rings to create a computationally-efficient axisymmetric formulation. The concept of Rayner and Brand was expanded to include the generation of multiple spanwise rings, with strengths dependent on the bound circulation distribution of the rotor (figure 5), and thus the ability to capture the precise influence of the design variation along the rotor radius.

The model is a time-stepping unsteady method with several sub-steps between each blade pass, which emits a new vortex ring. The downwash velocity induced by every ring on an axisymmetric point of every other ring is computed using the Biot Savard Law, which is shown to be a straightforward and computationally efficient method of calculation (Ref. 19). The rings are displaced according to the downwash velocity, and the time stepping continues. The model was designed as an inverse design method where the distribution of the lift coefficient is the design variable instead of the geometric angle of attack of the rotor blades. This speeds convergence to the steady state solution (since the bound-circulation does not change as the solution progresses) and also allows for the elimination of aero-structural iterations.

One of the most important criteria was the ability of the model to accurately capture the effect of the ground plane, which was validated against several well developed models shown in figure 6. The model was configurable for various levels of fidelity: HF (High Fidelity) uses 15 spanwise elements or 15 emitted vortex rings, 5 sub steps between ring emission, and 40 elements in the discretization of each ring for numerical integration. In comparison, LF (Low Fidelity) uses 5, 1, and 15, which is shown to be insufficient. HF and MF settings were used for all optimizations.

The structural model utilized a 1-dimensional frame-element finite element model (12-degree-of-freedom) to determine the deflection and stresses in the rotor spar. This was coupled with a failure prediction scheme including composite laminate failure and empirical estimations of non-linear failure modes (e.g. shell buckling) developed previously for the *Snowbird* (Ref. 10). A detailed parametric mass estimation model for the rotor was developed based on mass data from *Snowbird*. Estimated masses and data from prior HPH attempts were used for the airframe structure and mechanical weights.

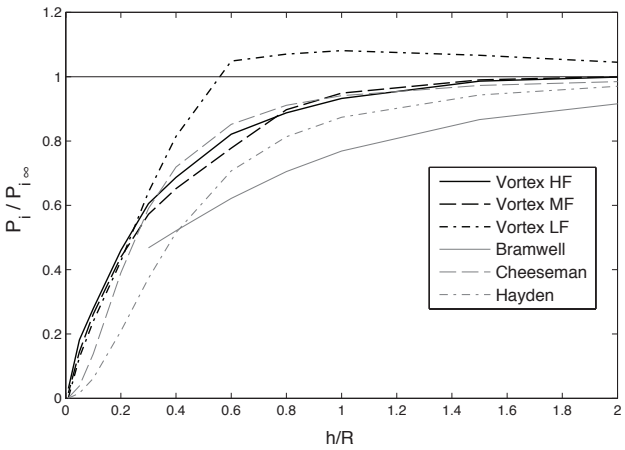


Fig. 6. The reduction in induced power at low altitude is shown using the blade-element model with various ground effect models, as well as the vortex-ring model, using various levels of fidelity.

Since the aerodynamic advantages of ground effect are somewhat diminished when the rotor blades deflect upwards during flight, finding the optimal balance between rotor stiffness and rotor weight requires a multidisciplinary aero-structural model. An inverse design approach was used here as well, since it would allow for an aero-structural solution that does not require iteration between the disciplines, and it would produce globally smooth output functions that are appropriate for gradient-based optimization. In the inverse design method, the distribution of the lift coefficient becomes the design variable, from which a simple blade-element model can give the lift forces required to compute the deflection of the structure in the out-of-plane direction. The vortex-ring model is then used to compute more accurate lift, drag and pitching moments. Finally, the full structural model computes the bending and twisting deflections, as well as the composite laminate failure criteria.

This 1-step pseudo-iteration requires only one call to the more computational expensive vortex-ring model and results in an output function that converged consistently and quickly when wrapped in a gradient-based optimization method. Design optimizations were performed using Matlab's `fmincon` function, with 20 to 30 design variables including the lift-coefficient distribution, chord distribution, spar diameter distribution, wrap angle of the carbon fibre, lift wire placement, chord wise length of leading-edge sheeting, etc. The multi-point optimization would look to minimize the required power, using a weighted average of the power at 3 *m* altitude and 0.5 *m* altitude, with the structural failure constraints based on a worst case control deflection case and a non-flying gravity-load case, where the rotors don't have the structural benefit of their bracing wire. An example of the comprehensive graphical interface used for `HeliCalc` during design is shown in figure 7.

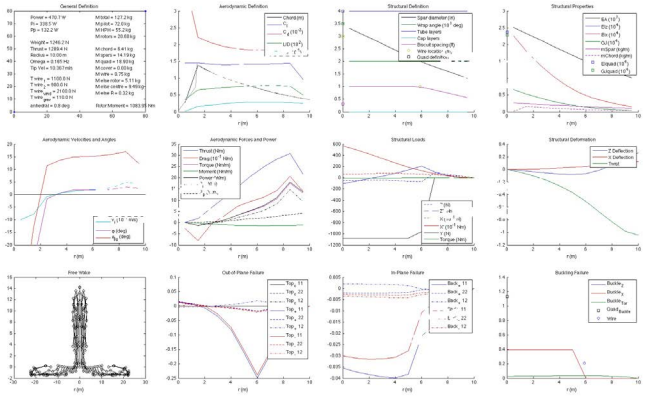


Fig. 7. Multi-pane graphical interface of the final `HeliCalc` optimization package.

Final Configuration Selection

A configuration trade-off between quad-rotor and reaction-drive single-rotor was performed using `HeliCalc`. Required power was determined for optimum-design helicopters with max dimension of 30, 40, 50, and 55 *m* (equal to 1 rotor diameter for the single-rotor, 2 rotor diameters for the quad-rotor). The two designs were again indistinguishable within error, and the optimal overall size, for a pilot weight of 170 *lbs*, was determined to be 50 *m* max dimension (see figure 8).

A quad-rotor design with blade radius of 10 *m* was selected primarily for the following reasons:

1. The quad-rotor configuration provided manufacturing and design efficiencies because of bi-lateral symmetry (i.e. 4 or 8 copies of most major components);
2. The quad-rotor configuration was shown to be very stable (the single-rotor *DaVinci III* had appeared less so);
3. With shorter rotors aero-elastic concerns would be minimized;
4. Composite structure components would not exceed 10 *m* in length, roughly the size required for the *Snowbird* and a practical limit for infrastructure and methodologies that had been developed.

Final Rotor Design

The final rotor design was carried out with `HeliCalc`. The structure was comprised of a tapering cylindrical main spar with a lift-wire attaching at 60% span, as opposed to a fully-cantilevered design. This braced solution was especially important for taking full advantage of ground effect, by maintaining rotor proximity to the ground. Airfoil profiles were designed for the required C_l at each of 4 spanwise stations and blended in-between. Brian Eggleston custom designed these low Reynolds number sections from his own designs and those of the Daedalus HPA, with the objective of minimizing drag at the design lift coefficient. The planform and airfoils are shown in figure 9.

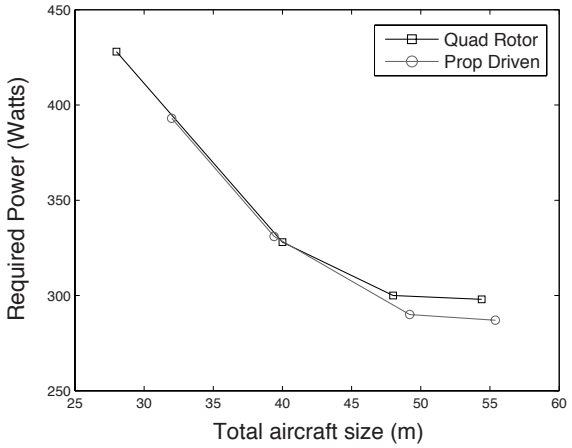


Fig. 8. Estimates of power required for quad rotor and single-rotor tip-driven configurations. Each point represents an aero-structural optimization using the blade-element model and Cheeseman and Bennett ground effect model.

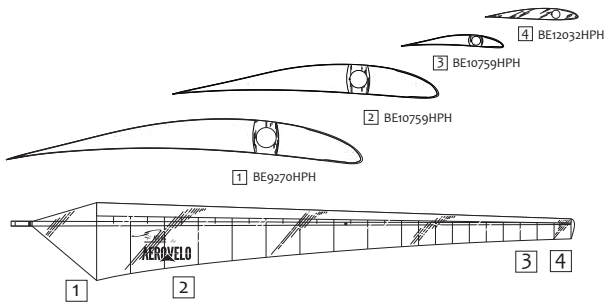


Fig. 9. Final optimized rotor planform and custom-designed airfoils for each station.

SYSTEM DESIGN & MANUFACTURE

Rotor Manufacture

The rotor structural design and aerodynamic surface geometry was determined using the optimizer `HeliCalc` as outlined above. The cylindrical shell spar was manufactured from high-modulus prepreg carbon fiber, which was axially wrapped around a conical mandrel and oven cured using hi-shrink tape for consolidation. Internal bulkheads of polystyrene foam and balsa wood were installed at 12" intervals to prevent shell buckling of the spar walls. The lift wire was initially made from Vectran line, selected for its high specific strength and resistance to creep under load. This was later changed to steel high-tensile strength piano wire for greater stiffness to better hold the rotor in ground effect, while not requiring a pre-tension that would have the rotors interfering with the ground during takeoff and landing. The rotor aerodynamic profile was built up using polystyrene foam ribs with balsa wood cap strips on the top and bottom surfaces, with CNC-cut polystyrene foam sheeting on the leading edge surface (to 15% chord) to maintain shape accuracy between ribs. The rotor was skinned with Melinex polyester film.

During spar production two full spars were chosen for destructive testing, the first of the production run as well as an example later that showed the greatest number of manufacturing defects. The first failed at a load less than predicted, but still above the estimated flight loads. The second failed very near the estimated flight loads, raising concern. The root cause was that the failure model had been developed for tubes with unidirectional reinforcement and hence greater thickness on the top and bottom surfaces. It had not therefore accurately captured compressive buckling of the thinner top face under bending load. This was exaggerated in areas of the tube where manufacturing defects had left localized gaps in the laminate. The defects were corrected as much as possible with extra plies on the exterior of the tube. Ultimately, only once during flight-testing did a rotor break in mid air due to an aerodynamic load that it had been designed to withstand, again ultimately due to a manufacturing defect (all other rotor failures were due to ground strikes). See figure 14 for further details on spar geometry and construction specifications.

Airframe

The main airframe structure was the focus of a protracted design process as it was expected to comprise 30% of the airframe mass and would determine much of the overall handling quality of the helicopter. Initial design concepts were aimed at structural efficiency, including the goal to avoid cantilevered structures, and if possible take advantage or wire-bracing to gain stiffness and design an arch-like configuration (where typically the foot of an arch transfers outward load to the ground abutment, here the load would be balanced by bracing lines to the opposite side of the structure). Furthermore, a design that was either truss-like or utilized long column members to transfer load from the rotors to the pilot would be ideal: structural members dominated by Euler column-buckling failure could be more accurately designed and would not be as susceptible to manufacturing defects.

The airframe design code was based on a finite-element analysis and failure prediction scheme (again 1-dimensional 12 degree-of-freedom frame-elements were used), coupled with a gradient-based optimizer (Matlab's `fmincon`). Two overall concepts were studied further: monolithic cylindrical booms with spreaders similar to a sailboat mast and external bracing, and a triangular-profile truss design. Both of these utilized cross-bracing from rotor to rotor to stiffen the overall structure, as well as lines in the ground plane of the structure to enable loading like an arch.

Further refinement of these two concepts showed the truss concept to be lighter-weight and higher rigidity (see figure 10). Critical load cases included opposed rotor control deflections (i.e. one blade increasing lift and the other decreasing), which with potential control strategies taking shape would be a potential mode of failure. In this particular case the differential in the two designs was substantial, though the deflection

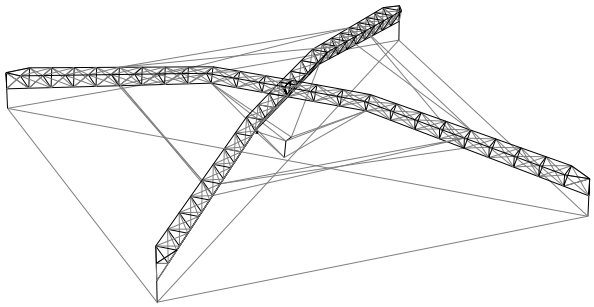


Fig. 10. Wireframe rendering of final truss design, with solid composite elements in black and lines in lighter gray.

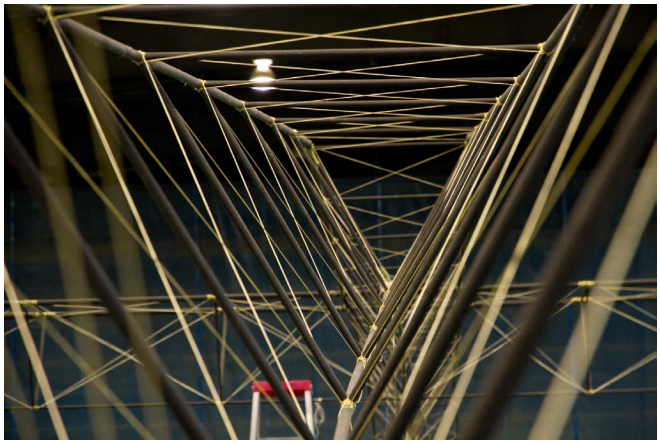


Fig. 11. Triangular-section string-based truss structure.

of the truss concept still seemed unrealistic (the accuracy of the model would be proven later in testing). Critical load analysis conducted at this time on wind-gust loads showed that the helicopter would not be tolerant of even minimal gusts (up to 2 *mph*), and outdoor flight was precluded as an option moving forward.

A unique aspect of the truss design was to use a minimal number of compression-capable members, and build much of the structure with pre-tensioned line (again Vectran for its zero-creep properties). The lines would carry all shear and torsion loads, as shown in figure 11). The longitudinal truss members and compression-bearing members were fabricated similarly to the rotor spar, but were of much smaller diameter and in some cases had a wall thickness at the minimum of the team's manufacturing capabilities.

Transmission & Cockpit

Design considerations for the power transmission and rotor drive system were primarily minimum-weight and no-slip locking of the relative rotor rotation. (Although *Atlas* was designed to have no rotor blade overlap, inspection of the *Yuri I* HPH videos showed that tip-vortex interaction was a likely cause of at least one major crash, and the capability to positively fix rotor phasing to minimize these interactions was

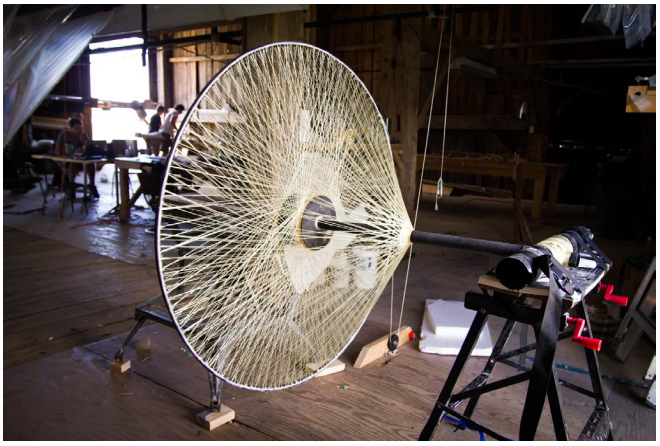


Fig. 12. Rotor hub inspired by a bicycle wheel, spoked with Kevlar yarn

desired).

Two concepts were evaluated. The first was spooled-line drive: string spooled at the rotor hub would be unwound from the hub and wound up at the pilot to drive the rotors. This strategy had been used by all previous successful HPHs and was very lightweight, though unfortunately was non-continuous and would require re-winding the helicopter after each flight. The other concept was for a continuous drive, either using a urethane/Kevlar toothed belt or a string with bonded beads/rungs functioning like a chain. After some investigation it was found that no continuous solution could be manufactured with sufficient strength at an acceptable weight.

The transmission spools were sized at a 10:1 ratio for a target pilot cadence of 100 RPM and rotor rotation of 10 RPM. Line spools at the pilot were custom designed and manufactured from carbon fiber, sized similarly to existing bicycle chainrings to take advantage of the commercial off-the-shelf (COTS) crankset provided. This required that the rotor-hub spools be larger in diameter (1.4 *m*) than is typically desired of a lightweight powertrain component. A bicycle wheel-inspired spoked concept was investigated, with a carbon fiber sandwich hub, Kevlar yarn spokes, and a carbon rim. Successive iteration rather than detailed structural modeling was pursued, and after 5 prototypes (successively addressing various buckling failure modes) a satisfactory design that weighed only 1 *lb* but sustained a drive-line tension of 150 *lbs* was developed (figure 12).

The cockpit configuration was selected as an upright bicycle versus recumbent as had been used by all three previous HPHs. From the authors' prior work in short-interval human-performance (designing and testing high-speed bicycles) and external consultations, the 60-second Prize flight required the sprint-power capability of an upright cycling configuration, whereas recumbent and upright configurations are equal for durations exceeding 5 minutes (Ref. 20). The upright bicycle frame (an R5ca from Cervelo Cycles) and the majority of the drivetrain were donated COTS components, selected for lightweight. A flywheel was chain-linked to the spools/cranks

to smooth pilot power input through the pedaling dead-spot and minimize oscillatory tensioning of the drivelines (which could be detrimental to the structural dynamics). This was a minimally-spoked bicycle rim and tire (with mass dictated by conveniently available COTS components), with maximum possible rotational inertia achieved by high gearing between the cranks and flywheel hub (a 5:1 ratio). The energy storage capability of the flywheel was negligible and thus did not violate the rules of the AHS competition. Electronic power-measurement pedals were installed on the bicycle cranks to collect power data in-flight.

Flight Controls

During control design the main points of consideration were counteracting of drift in flight, control of aircraft yaw, and the capability for collective (during climb and descent). Early on the need for yaw control was dismissed: with at least marginal consideration for torque balancing during control actuation, due to the helicopter's rotational inertia it seemed extremely unlikely that to aircraft would rotate 180 degrees in flight. Cyclic pitch/roll control (actuated simultaneously on all rotors) was considered, but most concepts used opposing-rotor differential lift to tilt the entire aircraft and thus the normal vector of each rotor's thrust. Differential lift methods evaluated and dismissed were RPM variation (which would make fixed rotor phasing impossible) and full-blade pitch changing. These systems were mechanically complex and required heavy bearings or mechanisms, as well as potentially requiring substantial actuation force from the pilot. The design team avoided control methods utilizing electronic actuation due to some ambiguity in the competition rules and the steep learning curve required in designing and implementing such a system.

Based on the authors' experience with aero-elastic tailoring of *Snowbird*, a concept was envisioned for aero-elastic collective. The blades of each rotor could be twisted or untwisted (washed-in or washed-out) from root to tip to provide more or less lift. All-flying canard surfaces would be mounted ahead of the spar on the rotor tips and actuated to provide a twisting torque. This solution was still somewhat mechanically complex with long actuation lines from the pilot to the canards (through a swashplate at the rotor hub), but required minimal pilot force and could be manufactured from lightweight components. A perceived added benefit was the induced drag reduction of the winglet and canard tip extensions, effectively increasing the rotor span by 15%. However, during flight-testing it was determined that the added lift required to counteract the canards (which in control-neutral position applied a downforce) and the substantial profile drag of the geometrically complex tip surfaces more than counteracted this benefit. A photo of the canard control surface is shown in figure 13.

Through mechanical mixing it would be possible to achieve both collective control (uniform changes across all four rotors) and pitch/roll control through opposing-rotor lift differential, but for low-altitude testing only pitch/roll control was implemented. By the time higher flights were required, *Gamera II's* testing had shown that collective rotor control was unnecessary for climb and descent and this feature was never implemented.



Fig. 13. Rotor-tip canard control surface.

Table 5. Atlas Specifications (June 2013)

Specification	Metric	Imperial
Diagonal Dimension Max	46.9 m	153.8 ft
Height Overall	3.6 m	11.9 ft
Rotor Radius	10.1 m	33.1 ft
Rotor Root Chord	1.4 m	4.6 ft
Rotor Tip Chord	0.3 m	1 ft
Actuator Disk Area	1281 m^2	13,789 ft^2
Rotor Speed	9.7 RPM	
Flight Power (0.5 m)	450 W	0.6 HP
Flight Power (3 m)	750 W	1.0 HP
Empty Weight	55.3 Kg	121.7 lb
All-Up Weight (with Pilot)	127.8 Kg	281.1 lb

The overall design of *Atlas* (as of August 2012) is shown in figure 14. *Atlas's* specifications (as of the June 13th 2013 Prize flight, not the August 2012 build completion) are given in table 5. *Atlas'* weight breakdown is given in table 6.

FLIGHT-TESTING & DEVELOPMENT

Initial Testing, Fall 2012

An indoor FIFA-regulation soccer field (*The Soccer Centre*) was found in Vaughan, Ontario that would accommodate flight-testing. Finding a large enough unobstructed indoor

Table 6. *Atlas* Mass Breakdown

Component	Metric [Kg]	Imperial [lb]
Rotor Blades	24.38	53.70
Rotor Hubs	6.91	15.21
Airframe/Truss Structure	19.23	42.36
Control Lines	0.12	0.26
Cockpit/Bike Frame	4.74	10.45
TOTAL	55.26	121.72

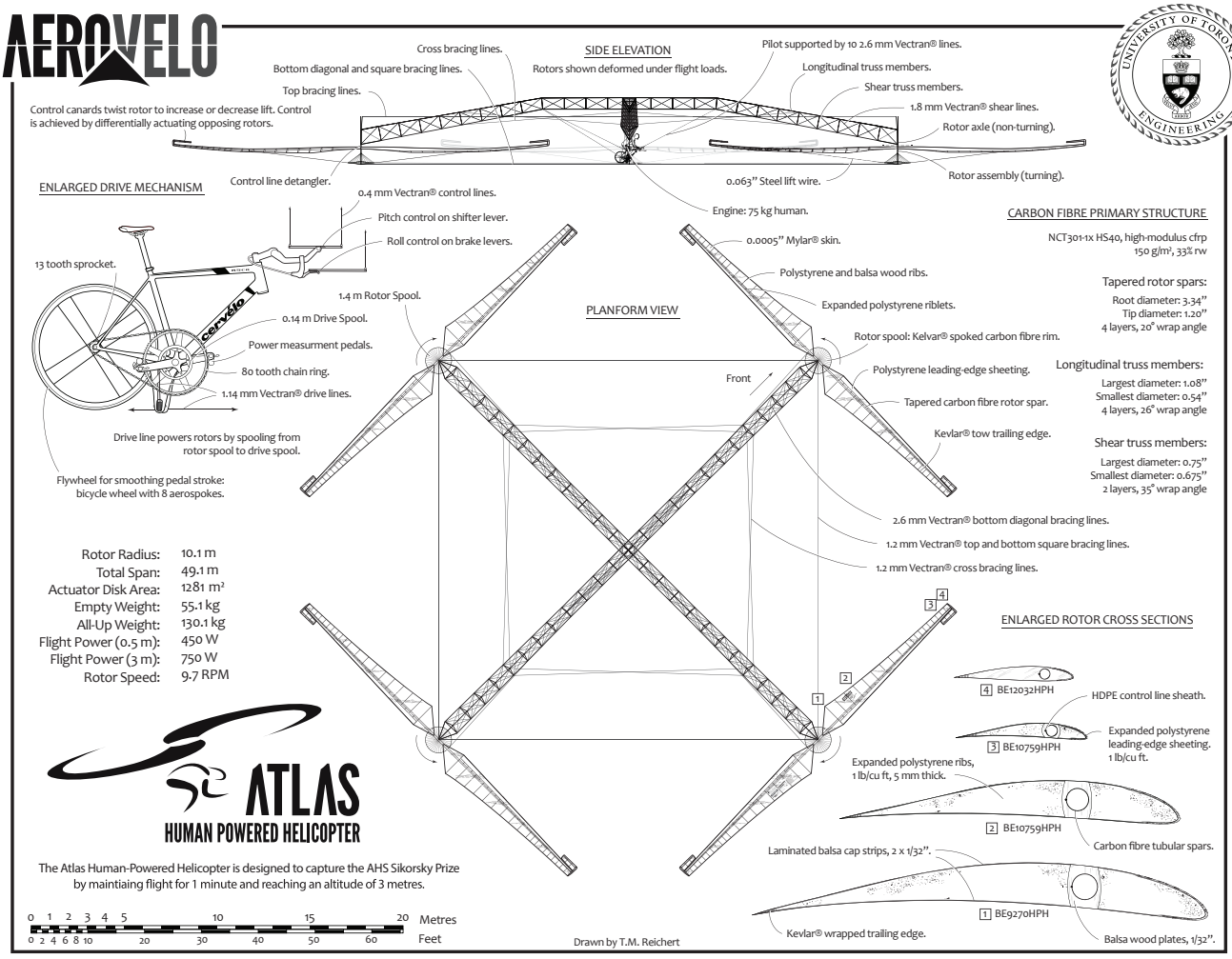


Fig. 14. Overall design of *Atlas* showing airframe structure with bracing lines, bicycle frame, and rotor arrangement. *Atlas* is shown here as configured in January 2013, later modifications included shorter truss arms (creating rotor overlap) and removal of the canard surfaces.

space was a significant challenge, and the high ceiling of the Soccer Centre was a benefit for reducing the likelihood that wake recirculation would become a concern over the course of the 60-second flight.

The first several days on the field focused on final integration of the airframe components and the sizing of bracing lines. When first the helicopter was entirely assembled, the team discovered that loading the pilot caused the structure to settle as each truss arm tilted over: the wire-bracing and truss lines were not nearly stiff enough. Further cross-bracing lines between each truss arm were added, and the pre-tension of many of the bracing lines, as well as of the truss lines was increased substantially. Tensioning of the truss lines in particular resulted in substantially changing the jig-twist of each arm, and more care was applied later in reversing this change and making further adjustments.

The helicopter was stored in a 53 ft trailer outside the facility to keep the field clear for recreational use. Typical flight operations involved assembling the aircraft in the early morning (2-3 hours), progressive flight-testing beginning with substantial re-trimming of the rotors each day (7 hours), then disassembling and re-packing the helicopter (1 hour) to be clear of 5pm soccer games.

The first session of flight-testing (two weeks in August-September 2012) showed progress from initial rotor spin-up to a first 4-second flight, culminating in a 17-second flight. The initial hope was that the Sikorsky Prize could be captured in this two-week session, but this quickly faded. By the end of this session the team had experience with assembly of the helicopter and typical flight operations, as well as trimming of the rotors (through root pitch adjustments) and canards for balanced flight. Some initial attempts at demonstrating control were also made, but ultimately with little result. During early testing there were numerous rotor spar failures from ground tip strikes, snagging on structural bracing lines, and in one case a manufacturing defect. In-situ repairs often allowed

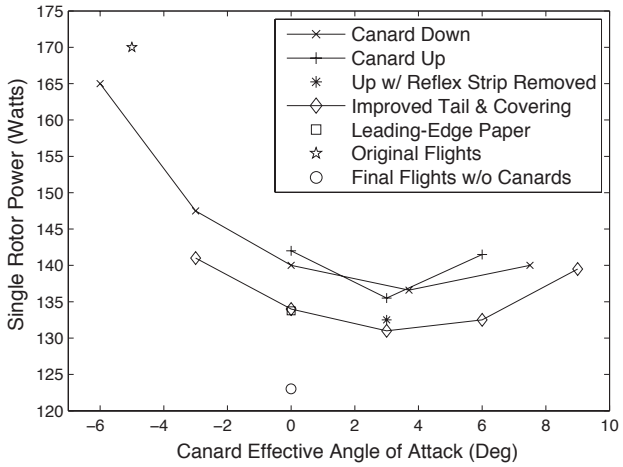


Fig. 15. The plot shows the progressive decrease in measured rotor power with improvements and angle of attack adjustments to the canards. The true single-rotor power is roughly 25 *W* less than shown, given that this amount of power is being drawn by the chain and flywheel. Substantial improvements were made by adjusting the canard angle of attack, removing the reflex strip at the trailing edge, improving the aerodynamic cleanliness, and finally removing the canards all together.

testing to resume the same day, each was a substantial weight increase (8% of blade weight per repair). Testing concluded when the student team returned to classes in the fall.

Experimental Optimization and Modifications

In the fall of 2012 the authors conducted systematic experimentation and modification to address many of the issues identified in initial testing. Of primary concern were opportunities for weight reduction and each component was evaluated for opportunities to simplify and shed mass via small modifications or substitution. A single-rotor whirl-stand was built to fly rotors independently for testing and experimental optimization. An experimental sweep was conducted of rotor pitch setting for minimum power, as the actual (versus modeled) extent of laminar flow and manufacturing accuracy's impact on profile drag were expected to effect the ideal rotor speed. See figure 15 for experimental studies of rotor power versus canard deflection setting.

Systematic improvement in operation of the canards was undertaken to address the concern of unbalanced actuation in flight. Bearing drag and control line friction improvements resulted in an 85% reduction in the overall control friction, leading to more precise and consistent control actuation. Steps were taken to re-jig and adjust the trusses after the significant line tensioning done during flight-testing. During flights the truss arms had been observed to twist significantly during changes in pilot power at roughly 1.5 degrees per 500 *W* of pilot input. Adjustments were made such that on the ground each rotor was slightly tilted, under low-altitude flight power the rotors would fly level, and under extreme climb power the rotors would over-tilt slightly. This truss twisting behavior (and the imparted tilting of the rotor thrust vectors) was a major cause of large dynamic oscillations of the helicopter structure under variation in pilot power.

Flight-Testing, 2013

Testing resumed in January 2013. Initial flight tests focused on adjusting the overall truss structure for improved stability in flight, as well as on the use of the canards for control. Flights of up to 30 *s* were achieved after four test sessions, but especially in longer flights it was apparent that the canards would not provide successful control. It was evident from video footage that upon ideal balanced actuation the canards would cause the desired aero-elastic effect and opposing rotor lift differential. However, in the first several seconds after actuation, the increased power in one rotor and decreased power in the opposite rotor caused a change in the two drive line tensions, bending the entire structure and tilting the rotor shafts (vectoring their thrust). Thus initially the helicopter would drift (due to thrust vectoring) in the direction opposite to the control input, then as the entire aircraft tilted due to lift differential finally drift in the intended direction would be achieved roughly 6-8 *s* after actuation.

Alternative control methods were investigated. Tests of cyclic actuation of the canards on a whirl-stand mounted rotor did not show any effect, likely due to the relatively short duration of the canard deflection given the slow dynamic response of the rotors. Drag brakes (in place of canards) were also proposed to cause power-induced thrust vectoring as seen before, without delayed secondary behavior. This would be prone to imbalanced actuation similar to the canards as well as a substantial power increase.

The ultimate solution was to directly tilt the rotor shafts to vector the thrust. Bracing lines that had formerly connected opposing rotors to transfer arch loads were rigidly fixed to the lowest point of the bicycle at the centre. Pilot lean front-back and left-right would move the centre-point of each bracing line, displacing the bottom of each rotor shaft and tilting the rotor. In initial proof tests this showed instantaneous response and sufficient control authority. Removal of the canards and associated components resulted in roughly 10% saving in total aircraft weight, substantial savings in profile/parasite drag, and a total of reduction in required power of nearly 20%.

Progressive testing at increasing duration and altitude led to a Sikorsky Prize flight attempt on March 15th, which ended in a mid-air breakup and crash from nearly 3 *m* in height. Video analysis showed that during initial descent form altitude one rotor dropped rapidly and pulled the adjacent rotor truss apart via bracing lines. Root cause of the rapidly falling rotor could not be determined with certainty from video evidence, but it was suspected that a drive-line spooling irregularity (either at the rotor hub or at the bicycle) had caused a loss of power. Procedures were implemented to ensure more consistent line spooling at the hubs, so that lines could not slip or



Fig. 16. *Atlas* flown by Todd Reichert on the AHS Sikorsky Prize-winning flight.

drop, and modifications were made to the bicycle line spooling system to ensure more consistent line stacking. The truss structure was repaired from the damaged components without re-manufacture of any components (hence at a weight cost) and without substantial modifications.

Atlas was flown again on April 18th and 19th, progressing from initial rotor trim and truss-adjustment flights to a 3 m-altitude Sikorsky Prize attempt by the end of the second day. Again the result was a catastrophic crash, with the same single rotor dropping precipitously upon descent from altitude. Confident that a line drop was not at fault, in a survey for likely root cause vortex-ring state was evaluated. In both of the major crashes, the sudden drop of the offending rotor occurred several seconds into the decent of the aircraft. The very low inflow velocity, in the range of 0.5 - 0.8 m/s at 3 m altitude, exacerbated by a rapid dive of one blade (caused by torsional oscillation of the truss arm), pointed to vortex-ring state as the most probable cause (and likely the cause of the previous crash).

The helicopter was repaired with extensive modifications and weight reduction consideration (repair weight was becoming a serious concern). The truss arms were shortened by 1.1 m to reduce weight, reduce torsional compliance, and avoid having to fabricate new carbon tubes (several sections were damaged beyond repair). Bracing lines were reconfigured to improve overall stiffness and reduce structural oscillations in flight under power variation. Aerodynamic refinements were made to the rotors to reduce overall power, and the blade pitch setting was again optimized (this had not been done since removing the canard controls).

Testing resumed for 5 days in June. Improved tuning of the structure and rotors, as well as consistent flight performance and control up to 2m flights led to an attempt on the AHS Sikorsky Prize on June 13th. The power profile was chosen such that the descent rate would be absolutely minimized, resulting in a rapid 12 s climb, followed by a slow 52 s descent. This flight was finally successful, reaching 3.3 m, remaining aloft for 64 s, and remaining within the required 10 m by 10 m box. The final flight at peak altitude is shown in figure 16.

Remarks on Flight Performance and Future Work

Future Analysis is required to correlate the aerodynamic model used to design *Atlas*, but some general comments can be made. The final aircraft weight despite all modifications was exactly as estimated, critical for success of an HPA. In addition, the final power available from the pilot-engine was within the estimated range required. Power measurements throughout testing showed that low-altitude hover power was roughly 25% higher than expected, whereas higher-altitude power (at 3 m) was very close to that predicted.

Based on this data and lessons learned during construction and testing, an redesigned iteration of *Atlas* should be capable of substantially improved performance. If the hover power required could be reduced to around 225 W, high-calibre human-powered aircraft pilots have been capable of this output (below their aerobic threshold) continuously for several hours (Ref. 21). In addition to a new airframe of reduced weight (*Atlas* final weight is comprised of 5-10% of repairs), the authors have developed concepts for lightweight continuous drive systems, rotor aerodynamic improvements (especially for profile drag), improved airframe and rotor structure design that should make this power reduction possible. The team at University of Maryland that designed and built the improved *Gamera II* achieved a 44% reduction if required power from *Gamera I*, showing that a 50% reduction in power for *Atlas* (from 450 W to 225 W) would not be unprecedented (Ref. 8). Other limiting factors such as structural dynamics and blade aerodynamic balancing encountered during testing of *Atlas* would certainly be detrimental to endurance flight but are surmountable.

CONCLUSION

The *Atlas* human-powered helicopter was successful in winning the AHS Igor I. Sikorsky Human-Powered Helicopter competition. Designed by a small team of graduate engineers and undergraduate students, the Atlas embodied creative design and innovative approaches, as well as analytic rigor and engineering. Novel aerodynamic analyses and multidisciplinary design strategies have been presented which are largely responsible for the lightweight structure and the incredible efficiency of *Atlas*, and that could be applied to configuration design of commercial helicopters. Future correlation of flight test data with model predictions would improve the value of these aerodynamic methods especially. Flight-testing showed that human-powered aircraft encounter many problems unique to this category of vehicle, as well as some well-known to conventional helicopters.

For the authors and project team the greatest benefits have been valuable engineering design experience and the impact of this accomplishment on the public and youth globally, inspiring many to think differently and challenge the impossible.

ACKNOWLEDGEMENTS

The *Atlas* Human-Powered Helicopter project would not have been possible without the passionate and dedicated student team members responsible for much of the design and fabrication of the aircraft. Support from friends, family, and community was crucial during development and flight-testing. The authors would also like to thank the generous corporate sponsors, foundations, organizations, and public donors without whom the *Atlas* could not have been built. Finally, this effort would not have been possible without the vision of the American Helicopter Society and Sikorsky Aircraft in fostering innovation and education with the creation and sponsorship of the AHS Igor I. Sikorsky Human-Powered Helicopter Competition.

REFERENCES

[1]Drees, J., "The Human-Powered Helicopter Challenge," *Vertiflite*, Vol. 39, (1), 1993, pp. 32–34.

[2]Jackson, P., "Prize in Human-Powered Helicopter Contest Rises to $250,000 Thanks to Sikorsky Aircraft Pledge," Sikorsky Aircraft Press Release, August 2009.

[3]Tarascio, M. J., "AHS Igor I. Sikorsky Human Powered Helicopter Competition," Website, vtol.org/awards-and-contests/human-powered-helicopter/hph-rules, January 2012.

[4]Lehoux, G., "Human Powered Helicopters: The History, The Technology, The People," Website, http://www.humanpoweredhelicopters.org/, January 2012.

[5]Larwood, S. and Saiki, N., "Aerodynamic Design of the Cal Poly Da Vinci Human-Powered Helicopter," American Helicopter Society Vertical Lift Design Conference, San Francisco, CA, January 1990.

[6]Sopher, R., "The AHS Igor Sikorsky Human Powered Helicopter Competition," *Vertiflite*, Vol. 43, (3), 1997, pp. 32–34.

[7]Schmaus, J., et al, "Design and Development of *Gamera*: A Human Powered Helicopter from the University of Maryland," American Helicopter Society Future Vertical Lift Aircraft Design Conference, San Francisco, CA, January 2012.

[8]Berry, B., et al, "Design Optimization of *Gamera II*: a Human Powered Helicopter," American Helicopter Society 68th Annual Forum, Fort Worth, TX, May 2012.

[9]Reichert, T., "Kinematic Optimization in Birds, Bats, and Ornithopters," PhD Thesis, Institute for Aerospace Studies, University of Toronto, November 2011.

[10]Robertson, C. D., "Structural Characterization, Optimization, and Failure Analysis of a Human-Powered Ornithopter," MASc Thesis, Institute for Aerospace Studies, University of Toronto, November 2009.

[11]Veitch, T., "An Unsteady Vortex Lattice Method for the Calculation of Aerodynamic Forces on Multi-Jointed Flexible Wings," BASc Thesis, Division of Engineering Science, Faculty of Applied Science and Engineering, University of Toronto, April 2008.

[12]Bramwell, A., Done, G., and Balmford, D., *Bramwell's Helicopter Dynamics, 2nd Ed.*, Butterworth-Heinemann, Oxford, UK, 2001, pp. 11–59.

[13]Tamai, G., *The Leading Edge*, Bentley, Cambridge, MA, 1999, pp. 31–80.

[14]The Peak Centre for Human Performance, "Specific Power Measurements of Various Cyclist Categories," Data Obtained via Email Correspondence, January 2012.

[15]Cheeseman, I. and Bennett, W., "The Effect of the Ground on a Helicopter Rotor in Forward Flight," British Aeronautical Research Council Report 3021, 1957.

[16]Hayden, J., "The Effect of the Ground on a Helicopter Rotor," American Helicopter Society 32nd Annual Forum, Washington, DC, May 1976.

[17]Rayner, J. M. V., "A Vortex Theory of Animal Flight: The Vortex Wake of a Hovering Animal," *Journal of Fluid Mechanics*, Vol. 91, 1979, pp. 697–730.

[18]Brand, A., Dreier, M., Kisnor, R., and Wood, T., "The Nature of Vortex Ring State," American Helicopter Society 63rd Annual Forum, Virginia Beach, VA, May 2008.

[19]Yoon, S. S. and Heister, S. D., "Analytical Formulas for the Velocity Field Induced by an Infinitely Thin Vortex Ring," *International Journal for Numerical Methods in Fluids*, Vol. 44, 2004, pp. 665–672.

[20]Whittingham, S., "Discussion of Human Power Capability Versus Duration," Live Interview at ASME HPV Challenge, April 2011.

[21]Langford, J. S., "The Daedalus Project: A Summary of Lessons Learned," Proceedings of the AIAA/AHS/ASEE Aircraft Design, Systems, and Operations Conference, 31 July - 2 August, 1989.

COPYRIGHT STATEMENT

The author(s) confirm that they, and/or their company or organisation, hold copyright on all of the original material included in this paper. The authors also confirm that they have obtained permission, from the copyright holder of any third party material included in this paper, to publish it as part of their paper. The author(s) confirm that they give permission, or have obtained permission from the copyright holder of this paper, for the publication and distribution of this paper as part of the ERF2014 proceedings or as individual offprints from the proceedings and for inclusion in a freely accessible web-based repository.